



# INFLUENCE OF REDUCTION OF DYNAMIC SHEAR MODULUS ON SEISMIC TENSILE STRESS OF ARCH DAM

Yoshiaki ARIGA<sup>1</sup>

<sup>1</sup> Member, Dr. Eng., Graduate School of Science and Technology, Hirosaki University,  
Aomori, Japan, y-a-arig@hirosaki-u.ac.jp

**ABSTRACT:** To verify the seismic performance of arch dams, it is necessary to evaluate the tensile stress caused by earthquake motion. When evaluating against strong earthquake motion, it is essential to consider the non-linearity of dynamic deformation property of dam. However, there is not much research on the effects of non-linear dynamic deformation property on seismic stress. The three-dimensional dynamic analysis was carried out to examine the impact on the seismic tensile stress when there is a reduction in dynamic shear modulus. The results show that both dynamic shear modulus and seismic tensile stress decreased at the most parts of the dam, but show an increase at the dam crest and abutment. In regard to seismic performance verification of arch dams, it should be noted that the seismic tensile stress may increase in some parts of dam by considering the non-linearity of dynamic shear modulus.

**Keywords:** *Seismic performance verification, 3-D dynamic analysis, Strain dependence, Arch dam, Tensile stress*

## 1. INTRODUCTION

Regarding the non-linearity of the dynamic deformation property of concrete dam, it shows that the dynamic shear modulus decreases and the damping factor increases according to the dynamic strain caused by earthquake motion. However, there is not much research on the quantitative evaluation of the values of the non-linearity. Therefore, the investigation on the strain dependence of the dynamic shear modulus on the dam was carried out by the three-dimensional reproduction analysis for the actual earthquake behavior of the existing arch dam. Furthermore, by utilizing these results, this research investigates the influence of non-linearity of dynamic shear modulus on the seismic stress on the dam by three-dimensional dynamic analysis.

## 2. RESEARCH BACKGROUND AND PURPOSE

The current seismic design of the dam is based on the seismic coefficient method, specified on the structural ordinance for river management facilities and the enforcement regulations<sup>1)</sup> in Japan. After the 1995 Southern Hyogo Prefecture Earthquake, the research on seismic performance was investigated by

dynamic analysis. The number of reports on the seismic performance verification method was published; the report on advanced research for seismic design of dams<sup>2)</sup>, the guidelines for seismic performance evaluation of dams during large earthquakes (draft)<sup>3)</sup> and the technical note on seismic performance evaluation of dams against large earthquake<sup>4)</sup>.

For the strength of dam concrete, it has low tensile strength. The tensile fracture is the strictest condition for the stability of the concrete dam. Furthermore, tensile stress is the most crucial indicator for seismic performance verification of concrete dams. The non-linearity of the dam needs to be considered when verifying against strong earthquake motion.

The non-linearity of the dam can be divided into a material non-linearity and a structural non-linearity. As for the material non-linearity, the strain dependence of dynamic shear modulus and damping factor, and the research based on the laboratory tests<sup>5)</sup>, the earthquake observation data<sup>6)</sup>, the numerical analysis for actual earthquake behavior<sup>7)</sup>, have been reported. Regarding the effects of the material non-linearity on the seismic stress, the results focus on the dynamic shear modulus<sup>8)</sup> and the damping factor<sup>9)</sup>. For the structural non-linearity, both investigation results and observation records<sup>10)</sup> show discontinuous behaviors at contraction joints and peripheral joints placed in the dam. Moreover, the results on numerical analysis using joint element<sup>11), 12)</sup>, the crack growth analysis<sup>13)</sup>, were also reported.

The mechanisms of the material non-linearity and the structural non-linearity differ. Therefore, the analysis method and evaluating made are also different. The values of dynamic deformation property have direct impacts on the deformation and displacement. However, the impacts on the stress are unclear. Due to that, the research focuses on material non-linearity and its impacts of the dynamic shear modulus on the seismic tensile stress.

### 3. EVALUATION OF STRAIN DEPENDENCE OF DYNAMIC SHEAR MODULUS BY THREE-DIMENSIONAL REPRODUCTION ANALYSIS FOR ACTUAL EARTHQUAKE BEHAVIOR OF EXISTING DAM

#### 3.1 Overview

After the 1995 Southern Hyogo Prefecture Earthquake, the three-dimensional reproduction analysis for the actual earthquake behaviors of existing dams was carried out by using the observed earthquake records, and the values of dynamic shear modulus and the damping factor for the existing dams were identified. Furthermore, the research and development of the practical method for seismic performance verification by three-dimensional dynamic analysis was executed<sup>14), 15)</sup>.

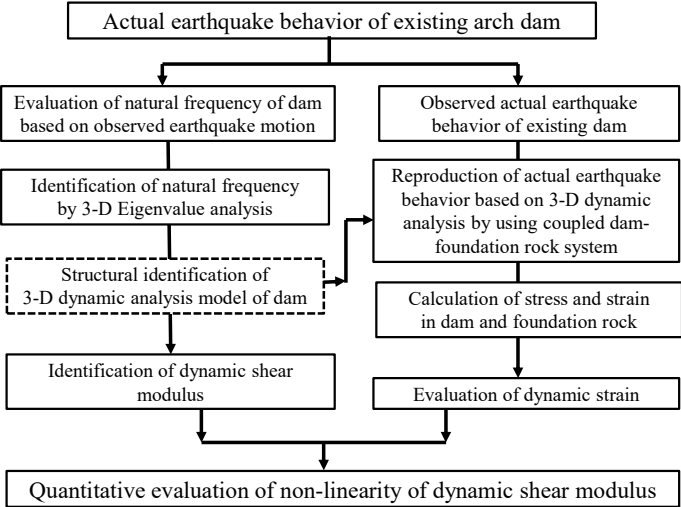


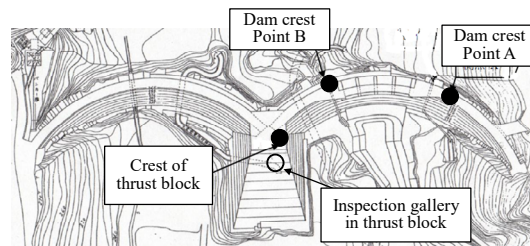
Fig. 1 Flow of evaluation for strain dependence of dynamic shear modulus of actual dam

In the previous studies, the acceleration levels of observed earthquake motions were small, so only the identification of dynamic shear modulus for small strain level was possible. However, in the 2011 off the Pacific Coast of Tohoku Earthquake, the strong earthquake motions with large acceleration were observed, which made it possible to evaluate the dynamic shear modulus for large strain level<sup>16)</sup>. Consequently, it became possible to evaluate the strain dependence of dynamic shear modulus<sup>17), 18)</sup>.

Figure 1 shows the flow of evaluation for the strain dependence of dynamic shear modulus of actual dam. The strain dependence of dynamic shear modulus can be evaluated by two processes, one is the evaluation for dynamic shear modulus and the other is for dynamic strain. First, the primary natural frequency of the dam was evaluated based on the spectra of acceleration time history. Then, the dynamic shear modulus was identified so that the primary natural frequency could be reproduced by three-dimensional eigenvalue analysis. The dynamic strain was evaluated by the three-dimensional dynamic analysis using the structurally identified analysis model. The curve of strain dependence of dynamic shear modulus was drawn by plotting the dynamic shear modulus on the vertical axis and the maximum tensile strain on the horizontal axis.

### 3.2 Evaluation of natural frequency of dam body

Figure 2 shows the arrangement of seismometers in the existing arch dam where the strong earthquake motions were observed during the 2011 off the Pacific Coast of Tohoku Earthquake. This dam is a double curvature arch dam in which two arch dams are connected by a concrete thrust block. The maximum dam height is 82 m (the heights of the right and left arch dams are 42 m and 82 m, respectively), and the total crest length is 323 m. The acceleration time histories as shown in Fig. 3 were observed during the main-shock on March 11, 2011<sup>19)</sup>. The maximum acceleration ( $A_{max}$ ) observed at point B at dam crest was 626 Gal ( $\text{cm/s}^2$ ) in the NS component. The power spectra of acceleration time histories observed at points A and B are shown in Fig. 4.



Strong earthquake motions were observed during the 2011 off the Pacific Coast of Tohoku Earthquake

Fig. 2 Arrangement of seismometers

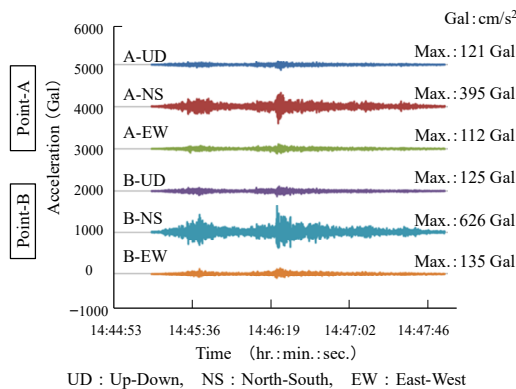


Fig. 3 Earthquake motions observed during the 2011 off the Pacific Coast of Tohoku Earthquake (March 11, 2011)

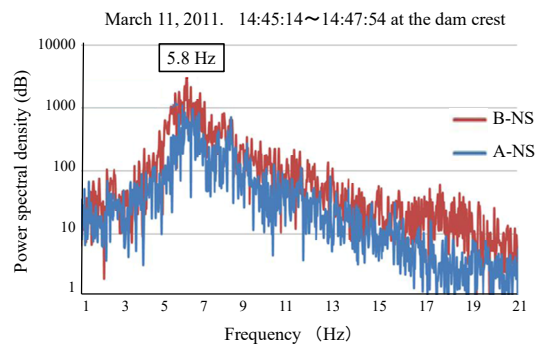


Fig. 4 Power spectra of earthquake motions observed at point A & B during the 2011 off the Pacific Coast of Tohoku Earthquake

To accurately evaluate the natural frequency of dam body, the frequency response function between the dam bottom and the dam crest is effective. However, since the seismic observation data at the dam bottom was not obtained, the power spectra at dam crest were used for evaluating the natural frequency of dam body. As shown in Table 1, the primary natural frequency of dam body ( $f_{pn}$ ) was 5.8 Hz during the main shock on March 11, 2011 with  $A_{max}$  of 626 Gal. Similarly,  $f_{pn}$  was 6.4 Hz during the aftershock on April 7, 2011 with 430 Gal<sup>20)</sup>, and 7.2 Hz during weak earthquake motion with several Gal.

Table 1 Primary natural frequency of dam body evaluated based on the observed earthquake motion during the 2011 off the Pacific Coast of Tohoku Earthquake

Level of earthquake motion	Primary natural frequency	Remarks (Gal = cm/s <sup>2</sup> )
Strong motion	$f_{pn} = 5.8$ Hz	Main shock (Max. Acc. = 626 Gal)
Medium motion	$f_{pn} = 6.4$ Hz	Maximum after shock (Max. Acc. = 430 Gal)
Weak motion	$f_{pn} = 7.2$ Hz	Weak motion (Max. Acc. = Several Gal)

### 3.3 Analysis model used for evaluating the strain dependence of dynamic shear modulus

Figure 5 shows the three-dimensional finite element model used for evaluating the strain dependence of dynamic shear modulus. This model was aimed to reproduce the actual earthquake behavior, so the shape and dimensions of dam was modeled as faithfully as possible to the existing dam. The analysis object is the double curvature arch dam with the total crest length of 323 m and the maximum dam height of 83 m. For the foundation rock, the region with a width of 450 m, a depth of 250 m and a height of 142 m was modeled. The dam and the foundation rock were modeled with the 8-node solid elements. A viscous boundary was set for the lateral boundary of foundation rock, and a rigid base for the bottom boundary. The number of nodes and elements of the model are 33,100 and 27,268, respectively.

The physical property values for analysis were set with reference to the results of reproduction analyses for actual earthquake behaviors of existing dams<sup>19)</sup>. The values of density, Poisson's ratio and damping factor of dam body were set to be 2.40 t/m<sup>3</sup>, 0.20 and 0.05, respectively. Based on the fact that the foundation rock is a hard rock composed of andesite and basalt, the values of dynamic shear modulus, density, Poisson's ratio and damping factor of foundation rock were set to be 4500 N/mm<sup>2</sup>, 2.60 t/m<sup>3</sup>, 0.25 and 0.05, respectively.

Regarding the reservoir water, the water level at the time of the 2011 off the Pacific Coast of Tohoku Earthquake was below the low water level. It is considered that the effect of reservoir water on the dam was small, so the reservoir water was omitted in this model.

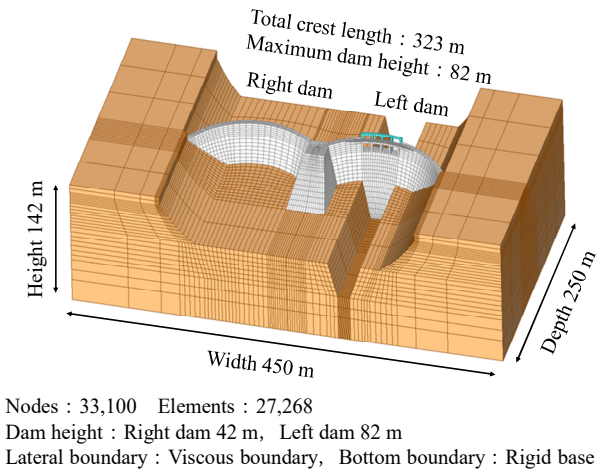


Fig. 5 3-D finite element model used for evaluating the strain dependence of dynamic shear modulus

The analysis was executed as a three-dimensional dynamic equivalent linear analysis by the time history response analysis based on the direct integration method. The analysis program ISCEF was used for the analysis.

### 3.4 Dynamic shear modulus of dam body identified by eigenvalue analysis

Table 2 shows the values of dynamic shear modulus of dam body ( $G_d$ ) identified by the eigenvalue analysis concerning  $f_{pn}$ , which was evaluated based on the observed earthquake data<sup>19)</sup>.  $G_d$  of 6000 N/mm<sup>2</sup> is the result identified by the eigenvalue analysis so that  $f_{pn}$  of 5.8 Hz is reproduced. Similarly,  $G_d$  of 7310 N/mm<sup>2</sup> and 9250 N/mm<sup>2</sup> are the identified results for  $f_{pn}$  of 6.4 Hz and 7.2 Hz. As  $A_{max}$  at the dam crest increased from several Gal to 430 Gal and 626 Gal,  $f_{pn}$  decreased from 7.2 Hz to 6.4 Hz and 5.8 Hz, and  $G_d$  decreased from 9250 N/mm<sup>2</sup> to 7310 N/mm<sup>2</sup> and 6000 N/mm<sup>2</sup>.

It is considered that this is not due to the structural non-linearity caused by the discontinuous behavior of joints, but due to the material non-linearity, that is the strain dependence of dynamic deformation property. There are two reasons for this. Firstly, according to the seismic response analysis for the 2011 off the Pacific Coast of Tohoku Earthquake, the maximum seismic tensile stress generated in the dam body was estimated to be about 1.22 N/mm<sup>2</sup>. At this level of seismic tensile stress, it could not be supposed that the discontinuous behavior at the joints occurred. Secondly, if the discontinuous behavior occurred at the joints, the seismic strain should be released and no decrease in  $f_{pn}$  should be seen. However, the decrease in  $f_{pn}$  was confirmed. From this fact, it is considered that the dam body behaved as a continuous body against strong earthquake motion.

Table 2 Dynamic shear modulus of dam body identified by reproducing the primary natural frequency

Level of earthquake motion	Identified dynamic shear modulus	Shear wave velocity	Primary natural frequency	Maximum acceleration
Strong motion	$G_d = 6000$ N/mm <sup>2</sup>	1580 m/s	$f_{pn} = 5.8$ Hz	626 Gal
Medium motion	$G_d = 7310$ N/mm <sup>2</sup>	1730 m/s	$f_{pn} = 6.4$ Hz	430 Gal
Weak motion	$G_d = 9250$ N/mm <sup>2</sup>	1960 m/s	$f_{pn} = 7.2$ Hz	Several Gal

### 3.5 Calculation of dynamic strain by 3D dynamic analysis

Three values of  $G_d$  were identified for three acceleration levels, as shown in Table 2. Therefore, if the dynamic strain for each acceleration level can be evaluated, it becomes possible to obtain the relationship between  $G_d$  and the dynamic strain. Figures 6–7 show the evaluated results for the maximum principal stress and the maximum principal strain by the three-dimensional dynamic analysis when  $G_d = 6000$  N/mm<sup>2</sup>. The strain dependence of  $G_d$  shown in Figs. 10–12 was obtained by combining  $G_d$  shown in Table 2 and the maximum principal strain shown in Fig. 7. The maximum principal strain is a maximum tensile axis strain.

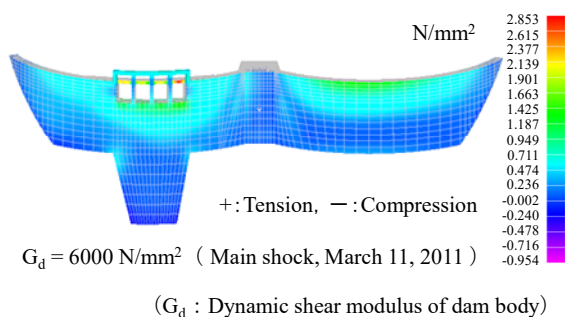


Fig. 6 Distribution of maximum principal stress when  $G_d = 6000$  N/mm<sup>2</sup>

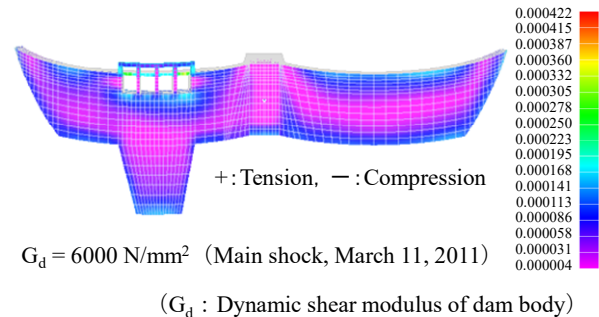


Fig. 7 Distribution of maximum principal strain when  $G_d = 6000$  N/mm<sup>2</sup>

The mode shapes of the 1st, 2nd, 3rd and 11th modes of dam body when  $G_d = 6000 \text{ N/mm}^2$  are shown in Fig. 8. The natural frequencies of the 1st, 2nd, 3rd and 11th modes were 5.79 Hz, 5.94 Hz, 6.03 Hz and 6.49 Hz, respectively. From Fig. 8, it can be seen that the displacement response of the left dam crest is noticeable in the 1st–3rd modes, and that the displacement response around the spillway at dam crest is prominent in the 11th mode.

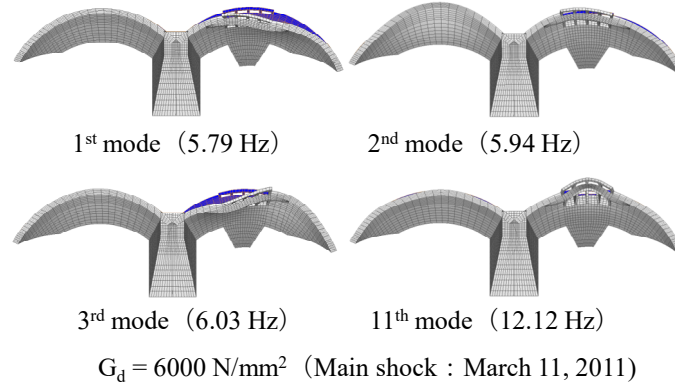


Fig. 8 Mode shapes and natural frequencies of dam body when  $G_d = 6000 \text{ N/mm}^2$

### 3.6 Evaluated results for strain dependence of dynamic shear modulus

Since the dynamic strain changed depending on the position of dam body, the representative positions were selected as shown in Fig. 9. The evaluated results of the strain dependence of  $G_d$  at the dam crest (position 1–2) are shown in Fig. 10. Similarly, the evaluation results at the dam center (position 3–4) and the dam bottom (position 5–6) are shown in Figs. 11 and 12, respectively.

Three green marks in the figure are the evaluated results for  $G_d = 9250 \text{ N/mm}^2$ ,  $7310 \text{ N/mm}^2$  and  $6000 \text{ N/mm}^2$ . The red curve is drawn to envelop them. The black marks and the black curve are the results based on the laboratory tension test<sup>5)</sup>. The vertical axis of the figure is the reduction rate ( $G_d / G_0$ ).  $G_0$  is the initial dynamic shear modulus. The horizontal axis is the seismic tensile axial strain ( $\epsilon_{st}$ ). The value of  $200 \mu$  was the limit strain when the tensile fracture occurred in the laboratory tension test.

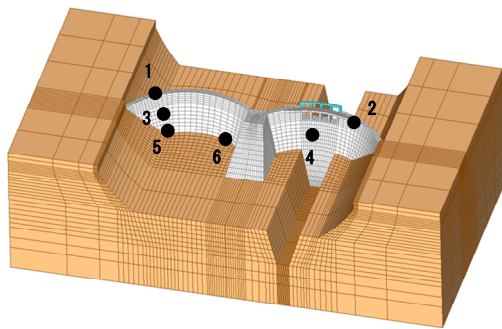
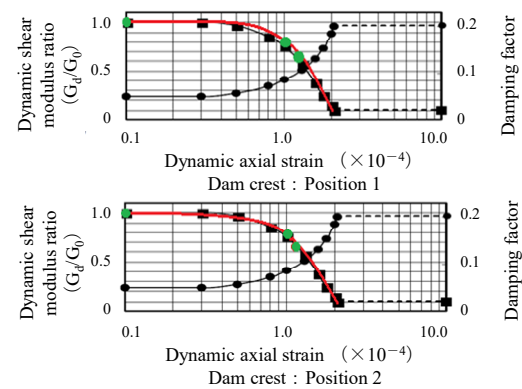


Fig. 9 Representative positions



$G_d$  : Dynamic shear modulus of dam  
 $G_0$  : Initial dynamic shear modulus of dam

Fig. 10 Strain dependence of dynamic shear modulus at dam crest (positions 1–2)

As shown in Figs. 10–12, the strain dependence of  $G_d$  can be confirmed at every representative position. Regarding the dam crest, the evaluated results were in good agreement with the results of laboratory tension test. However, as for the dam bottom,  $G_d$  decreased slightly earlier than the results of laboratory test. As for the center of dam,  $G_d$  decreased considerably earlier. The reason for this can be thought that the central part of dam is less deformable than the dam crest and the dam bottom.

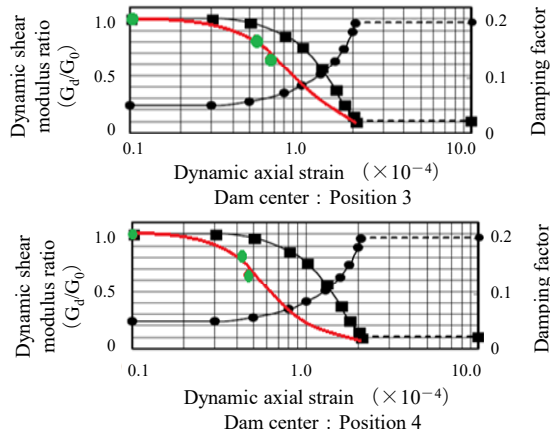


Fig. 11 Strain dependence of dynamic shear modulus at dam center (positions 3–4)

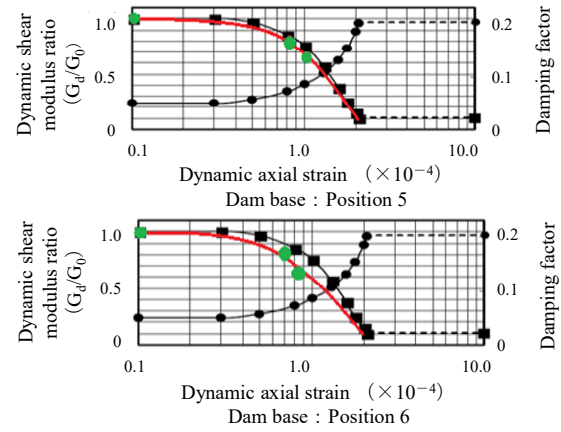


Fig. 12 Strain dependence of dynamic shear modulus at dam bottom (positions 5–6)

#### 4. EVALUATION OF IMPACTS OF REDUCTION IN DYNAMIC SHEAR MODULUS ON SEISMIC TENSILE STRESS

##### 4.1 Overview

In regard to the fill dams, there are many studies on the non-linearity of deformation property of dam material, and there is a lot of research on the impacts of the non-linearity of dynamic deformation property on the seismic response of dam. On the other hand, regarding the concrete dams, there are few studies on the non-linearity of the deformation property of dam material. And there are still unsolved issues regarding the impacts of the non-linearity of dynamic deformation properties on the seismic safety of concrete dams. Therefore, the impacts of reduction in dynamic shear modulus on the seismic tensile stress were investigated by conducting the three-dimensional dynamic analysis for the double curvature arch dam.

##### 4.2 Analysis object

The Hongrin Dam (dam height: 123 m, total crest length: 600 m, completion 1969, Switzerland) and the Okura Dam (dam height: 82 m, total crest length: 323 m, completion 1961, Japan) are known as the construction cases of double curvature arch dam. With reference to these existing construction cases, a double curvature arch dam with a height of 100 m was set as the analysis object.

##### 4.3 Analysis model

The three-dimensional analysis model is shown in Fig. 13. The purpose of this study is to investigate the impacts of changes in  $G_d$ , so the shape and dimensions of the model are simply idealized. The height of the dam is 100 m for both left and right dam. The crest length is 310 m for the right dam and 246 m for the left dam. The length of dam bottom is 166 m for the right dam and 100 m for the left dam. The shape of the dams are set to be asymmetric.

The thrust block is made of concrete, and the length of the top and the bottom is 50 m and 143 m, respectively. The dam and the foundation rock were modeled with the 8-nodes solid elements. The lateral boundary of the foundation is a viscous boundary and the bottom boundary is a rigid base. The element division of dam body in the depth direction is five layers so that the stress inside the dam body can be output. The number of nodes and elements are 24,529 and 13,460, respectively.

When the reservoir water is full, the compressive pressure by reservoir water acts on the surface of arch dam, and the dam becomes in a compressive stress condition. But, if there is no reservoir water, the compressive pressure due to the reservoir water does not act on the dam, so the tensile stress is likely to occur by strong earthquake motion. Therefore, the condition of reservoir water becomes more severe in the empty state than in the full state. So, it was assumed that there was no reservoir water.

The evaluation was performed by the three-dimensional dynamic linear analysis based on the direct integration method. The analysis program ISCEF was used.

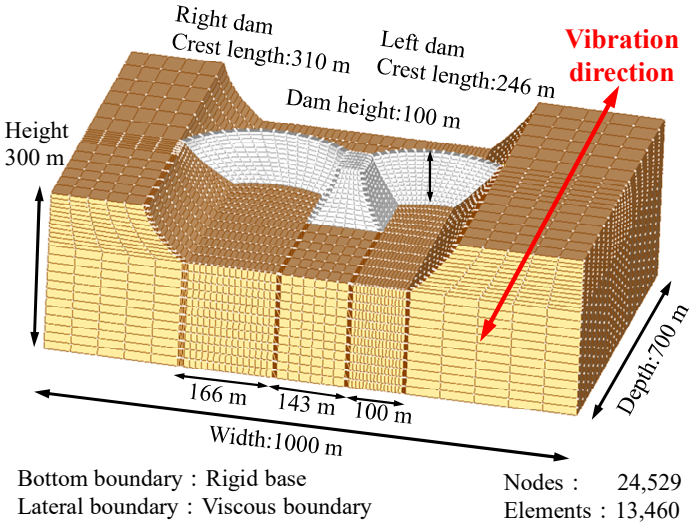


Fig. 13 3-D analysis model for investigating the impacts of changes in dynamic shear modulus

#### 4.4 Physical property values for analysis

The dynamic property values of dam body and thrust block are shown in Table 3. Three cases are set for  $G_d$ , assuming a weak earthquake motion level ( $G_d/G_0 = 1.0$ ), a medium earthquake motion level ( $G_d/G_0 = 0.73$ ) and a strong earthquake motion level ( $G_d/G_0 = 0.65$ ). The dynamic property values of foundation rock are shown in Table 4. The non-linearity (strain dependence) of dam body was set as shown in Fig. 14. The black square mark in Fig. 14 shows the results of laboratory tension test of dam concrete, and the three red circles indicate the results of three-dimensional reproduction analysis for existing double curvature arch dam during the 2011 off the Pacific Coast of Tohoku Earthquake<sup>19)</sup>.  $G_d/G_0$  was assumed as shown in Fig. 14 considering that the dam crest is the important part for dam safety. The damping factor was set to be 0.05 with reference to the results of the laboratory tension test of dam concrete<sup>5)</sup>.

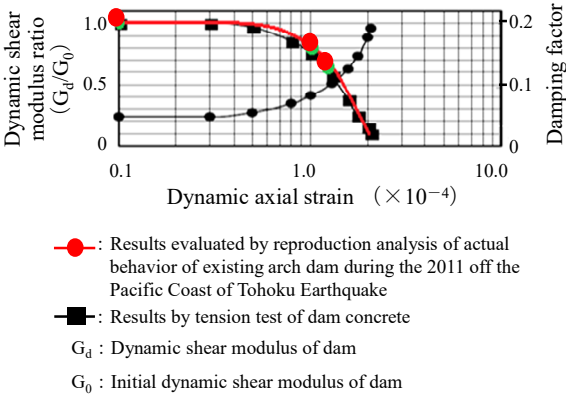


Fig. 14 Strain dependence of dynamic shear modulus of dam body



Table 3 Dynamic property values of dam body and thrust block

Analysis case	Identified dynamic shear modulus	Density	Poisson's ratio	Damping factor	$G_d/G_0$	Maximum acceleration
Case-1	$G_d = 9250 \text{ N/mm}^2$	$2.4 \text{ t/m}^3$	0.2	0.05	1.0	626 Gal
Case-2	$G_d = 7310 \text{ N/mm}^2$	$2.4 \text{ t/m}^3$	0.2	0.05	0.73	430 Gal
Case-3	$G_d = 6000 \text{ N/mm}^2$	$2.4 \text{ t/m}^3$	0.2	0.05	0.65	Several Gal

$G_d/G_0$  : Reduction rate for dynamic shear modulus,  $G_0$  : Initial dynamic shear modulus

Table 4 Dynamic property values of foundation rock

Dynamic shear modulus	Shear wave velocity	Density	Poisson's ratio	Damping factor
$4500 \text{ N/mm}^2$	1315 m/s	$2.6 \text{ t/m}^3$	0.25	0.05

#### 4.5 Input earthquake motion

The earthquake motion illustrated by the Japan Society of Civil Engineers shown in Fig. 15 was used<sup>21)</sup>, and the motion was input from the bottom rigid base in the up-downstream direction.

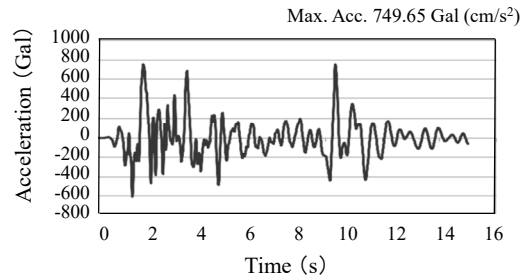


Fig. 15 Input earthquake motion<sup>21)</sup>

#### 4.6 Analysis results for seismic tensile stress in dam body

The maximum values of seismic tensile stress at the representative positions are shown in Table 5. The representative positions are as shown in Fig. 16. The seismic tensile stress ( $\sigma_{dt}$ ) shown in Table 5 is not the stress added to normal tensile stress, but the stress generated by the earthquake motion. The distributions of  $\sigma_{dt}$  in the dam body are shown in Fig. 17.

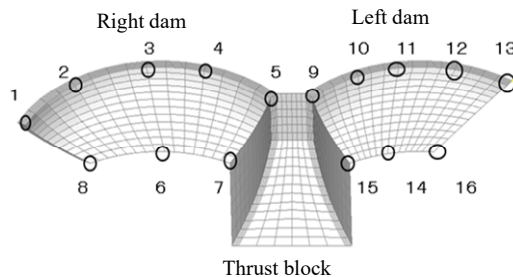


Fig. 16 Representative positions of dam body

At position 10 (near right bank at left dam crest),  $\sigma_{dt}$  was  $18.8 \text{ N/mm}^2$ ,  $21.9 \text{ N/mm}^2$  and  $23.9 \text{ N/mm}^2$  when  $G_d$  was  $9250 \text{ N/mm}^2$ ,  $7310 \text{ N/mm}^2$  and  $6000 \text{ N/mm}^2$ , respectively. Thus,  $\sigma_{dt}$  increased as  $G_d$

decreased. At positions 1 and 13 (right and left abutment), the values of  $\sigma_{dt}$  were small, and the changes in  $\sigma_{dt}$  due to the decrease of  $G_d$  were also small. At position 5 (connection between right dam crest and thrust block),  $\sigma_{dt}$  was 29.7 N/mm<sup>2</sup>, 27.0 N/mm<sup>2</sup> and 19.3 N/mm<sup>2</sup> when  $G_d$  was 9250 N/mm<sup>2</sup>, 7310 N/mm<sup>2</sup> and 6000 N/mm<sup>2</sup>, respectively. In this case,  $\sigma_{dt}$  decreased largely as  $G_d$  decreased. At position 9 (connection between left dam crest and thrust block),  $\sigma_{dt}$  was 32.6 N/mm<sup>2</sup>, 28.4 N/mm<sup>2</sup> and 29.7 N/mm<sup>2</sup> when  $G_d$  was 9250 N/mm<sup>2</sup>, 7310 N/mm<sup>2</sup> and 6000 N/mm<sup>2</sup>, respectively. The values of  $\sigma_{dt}$  were large and showed the downward tendency with the decrease in  $G_d$ . At position 3 (crest center of right dam) and position 12 (near left bank of left dam crest), the values of  $\sigma_{dt}$  were relatively large, and the downward tendency with the decrease in  $G_d$  was also relatively large.

Table 5 Maximum tensile stress caused by earthquake motion at representative positions

No.	Representative positions		Dynamic shear modulus of dam ( $G_d$ )			
			9250 N/mm <sup>2</sup>	7310 N/mm <sup>2</sup>	6000 N/mm <sup>2</sup>	
1	Right dam	Dam crest	Right abutment	11.3	9.0	11.2
2			Near right bank	24.8	23.3	22.4
3			Crest center	20.1	18.7	14.6
4			Near left bank	13.7	14.6	13.3
5			Thrust block connection	29.3	27.0	19.3
6	Crest length 310 m	Dam base	Bottom center	15.5	13.6	12.8
7			Thrust block connection	6.3	5.2	5.4
8			Right bank	8.8	8.3	7.6
9	Left dam	Dam crest	Thrust block connection	32.6	28.4	29.7
10			Near right bank	18.8	21.9	23.9
11			Crest center	7.2	6.8	7.1
12			Near left bank	32.1	28.7	26.6
13			Left abutment	19.6	20.4	17.7
14		Crest length 246 m	Dam base	Bottom center	14.6	13.2
15	Thrust block connection			7.6	6.1	5.8
16			Left bank	8.2	6.6	6.4

(unit: N/mm<sup>2</sup>)

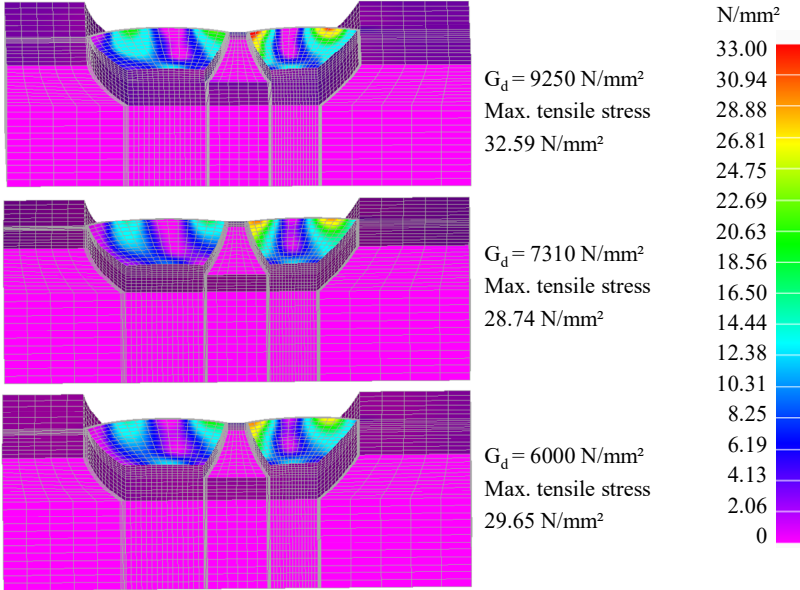


Fig. 17 Distributions of  $\sigma_{dt}$  in the dam body according to the change in  $G_d$

On the other hand, at position 11 (crest center of left dam),  $\sigma_{dt}$  was small, and the effect of decrease in  $G_d$  was small. As shown in Fig. 17, there was a slight difference in the distribution of  $\sigma_{dt}$ . While  $\sigma_{dt}$  tended to decrease at many positions as  $G_d$  decreased,  $\sigma_{dt}$  tended to increase at position 10 (near right bank at the left bank crest). In regard to this, it is considered that the vibration mode of a coupled dam-thrust block-foundation rock system changed due to the reduction in  $G_d$ , consequently  $\sigma_{dt}$  increased at the positions where the earthquake response changed. The mutual influence among the dam body, thrust block, and foundation rock is a subject for future study.

**4.7 Analysis results for seismic tensile stress in thrust block**

The distribution of  $\sigma_{dt}$  on the thrust block (upstream side) is shown in Fig. 18. Table 6 shows the maximum values of  $\sigma_{dt}$  at the representative positions shown in Fig. 19. At position 1 (upper part of right dam connection),  $\sigma_{dt}$  was 11.0 N/mm<sup>2</sup>, 9.3 N/mm<sup>2</sup> and 6.7 N/mm<sup>2</sup> when  $G_d$  was 9250 N/mm<sup>2</sup>, 7310 N/mm<sup>2</sup> and 6000 N/mm<sup>2</sup>, respectively. In the thrust block,  $\sigma_{dt}$  generally decreased as  $G_d$  decreased.

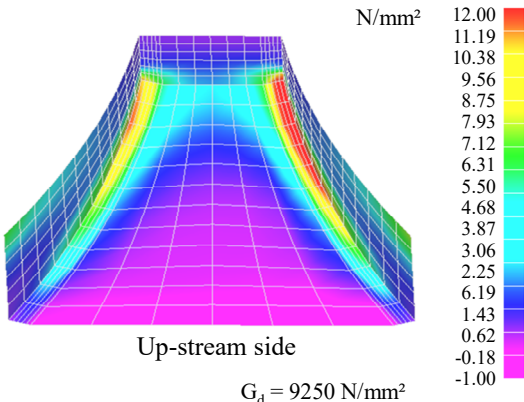


Fig. 18 Distribution of seismic tensile stress in the thrust block (upstream side)

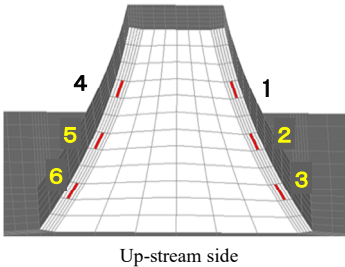


Fig. 19 Representative positions at the thrust block

Table 6 Maximum tensile stress caused by earthquake motion in the thrust block

No.	Representative positions		Dynamic shear modulus of dam ( $G_d$ )			
			9250 N/mm <sup>2</sup>	7310 N/mm <sup>2</sup>	6000 N/mm <sup>2</sup>	
1	Thrust block	Right dam connection	Upper part	11.0	9.3	6.7
2			Middle part	7.8	6.1	5.2
3			Lower part	4.4	4.0	4.0
4	Thrust block	Right dam connection	Upper part	10.1	8.6	9.1
5			Middle part	6.7	5.7	6.0
6			Lower part	4.8	3.9	3.8

(unit: N/mm<sup>2</sup>)

**4.8 Analysis results for seismic tensile stress in foundation rock**

The distribution of  $\sigma_{dt}$  in the foundation rock is shown in Fig. 20. Table 7 shows the maximum values of  $\sigma_{dt}$  at the representative positions shown in Fig. 21. The values of  $\sigma_{dt}$  at position 1 (upper right abutment) was 4.3 N/mm<sup>2</sup>, 4.3 N/mm<sup>2</sup> and 5.3 N/mm<sup>2</sup> when  $G_d$  was 9250 N/mm<sup>2</sup>, 7310 N/mm<sup>2</sup> and 6000 N/mm<sup>2</sup>, respectively. In the dam body and the thrust block,  $\sigma_{dt}$  generally showed a decreasing tendency as  $G_d$  decreased. However, in the foundation rock, there are some positions showing the increasing tendency. The seismic safety of arch dam largely depends on the soundness of foundation

rock. Therefore, the seismic performance should be very carefully verified when  $\sigma_{dt}$  increases in the foundation rock.

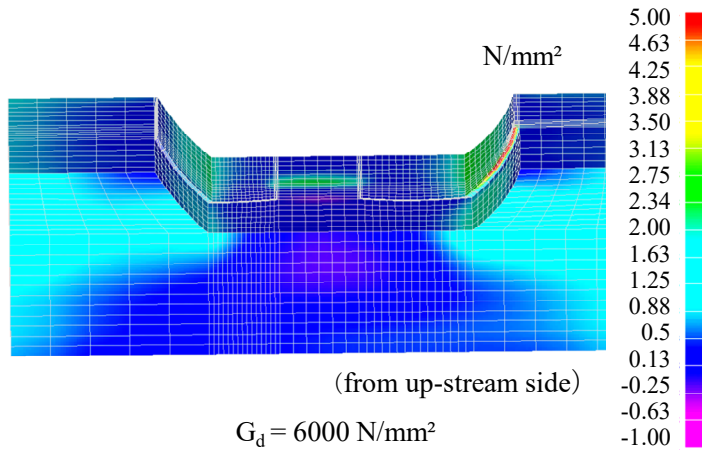


Fig. 20 Distribution of seismic tensile stress in the foundation rock

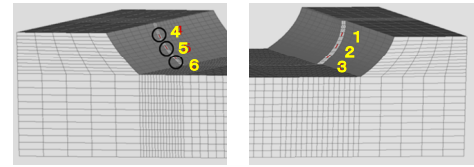


Fig. 21 Representative positions at the foundation rock

Table 7 Maximum tensile stress caused by earthquake motion in the foundation rock

No.	Representative positions		Dynamic shear modulus of dam ( $G_d$ )			
			9250 N/mm <sup>2</sup>	7310 N/mm <sup>2</sup>	6000 N/mm <sup>2</sup>	
1	Foundation rock	Right abutment of right dam	Upper part	4.3	4.3	5.3
2			Middle part	5.0	5.0	5.2
3			Lower part	4.7	4.6	4.6
4		Left abutment of left dam	Upper part	4.8	5.2	4.4
5			Middle part	3.5	3.9	3.5
6			Lower part	3.6	3.5	3.6

(unit: N/mm<sup>2</sup>)

## 5. CONCLUSIONS

This study proposed a method to evaluate the non-linearity of dynamic deformation property of concrete dam by utilizing three-dimensional dynamic analysis and the data gathered from the earthquake observation. This method was used to evaluate the strain dependence of  $G_d$  for the existing double curvature arch dam where the strong earthquake motions were observed in the 2011 off the Pacific Coast of Tohoku Earthquake.

Furthermore, the impacts of the decreasing in  $G_d$  on  $\sigma_{dt}$  generated in the dam body and foundation rock were investigated by the three-dimensional dynamic analysis. The results show that  $\sigma_{dt}$  generated in the dam body showed a decreasing trend at many positions as  $G_d$  decreases. However, some parts of dam crest and abutment showed an increasing trend even though  $G_d$  decreases.

The seismic safety of arch dam largely depends on the soundness of foundation rock. Therefore, if  $\sigma_{dt}$  increases in the foundation rock, the seismic performance should be carefully verified. In regard to the double curvature arch dam, when  $G_d$  decreases, the seismic behavior of coupled dam, thrust block, foundation rock system will be more complicated. So, it will be necessary to pay special attention to the connection parts between dam body, thrust block, and foundation rock.

When  $\sigma_{dt}$  decreases as  $G_d$  decreases, the seismic performance evaluation with no consideration on the non-linear effects will be on the safe side, but if  $\sigma_{dt}$  increases as  $G_d$  decreases, it will be on the danger side. Consequently, when  $\sigma_{dt}$  increases with the decrease of  $G_d$ , it is vital to carefully verify the seismic

performance.

To prevent and mitigate the structural damages by the earthquake, it is necessary to accurately verify the seismic performance for arch dams. The three-dimensional dynamic analysis is useful to carry out the seismic performance verification with high accuracy and reliability.

## 6. AFTERWORD

The increase or decrease in seismic tensile stress when the dynamic shear modulus decreases will depend on the shape and scale of dam, the dynamic deformation property of dam and foundation, the mutual influences between dam, foundation, and reservoir, the characteristics of earthquake motions, and so forth. Dam is a structure with strong site dependence, so it is necessary to accurately consider the characteristics for individual dams when conducting the seismic performance verification.

It should be noted that the larger and the more complex the dam is, the stronger the impacts of change in dynamic shear modulus become. For future study, it is necessary to examine the influences of reservoir water and sediment, and the impacts on the discharge facility located at the dam crest.

## ACKNOWLEDGMENT

The author would like to thank Mr. Hiroaki Nakagawa, Dr. Yoshiaki Ozawa, and Mr. Taku Yasue of Century Techno Inc. for their kind consideration and cooperation in using the analysis program ISCEF.

## REFERENCES

- 1) Structural Ordinance for River Management Facilities (Government Ordinance No. 199, 15 pp., July 1976) and Enforcement Regulations (Ministerial Ordinance No. 13, 14 pp., October 1976), 1976 (in Japanese).
- 2) Agency for Natural Resources and Energy, Ministry of Economy, Trade and Industry, Electric Power Civil Engineering Association: Report on Advanced Research for Seismic Design of Dams (2000 Research on Earthquake Countermeasures for Electric Power Facilities), 484 pp., 2001 (in Japanese).
- 3) River Bureau of the Ministry of Land, Infrastructure and Transport: Guidelines for Seismic Performance Evaluation of Dams during Large Earthquakes (draft), 26 pp., 2005 (in Japanese).
- 4) National Institute for Land and Infrastructure Management, Ministry of Land, Infrastructure and Transport: Technical Note on Seismic Performance Evaluation of Dams against Large Earthquake, *Technical Note of National Institute for Land and Infrastructure Management*, No. 244, 192 pp., 2005 (in Japanese).
- 5) Hatano, T.: Theory of Failure of Concrete and Similar Brittle Solid on the Basis of Strain, *Journal of Japan Society of Civil Engineers*, No. 153, pp. 31–39, 1968 (in Japanese).
- 6) Okuma, N., Mazda, T., Kanazawa, K. and Ikeda, K.: Seasonal Changes in Dynamic Properties of Two Large Arch Dams on Ambient Vibration Measurements, *Journal of Japan Society of Civil Engineers*, SER. A1 (Structural Engineering & Earthquake Engineering), Vol. 68, No. 4, pp. I\_883–I\_890, 2012 (in Japanese).
- 7) Sakamoto, H., Sato, N., Tomita, N. and Kusahana, K.: Dynamic Analysis and Three-Dimensional Seismic Behavior of the Arch Dam, *Journal of Japan Society of Dam Engineers*, Vol. 27, No. 1, pp. 26–35, 2017 (in Japanese).
- 8) Watanabe, H., Ariga, Y. and Cao, Z.: Earthquake Resistance of a Concrete Gravity Dam Revaluated with 3-D Nonlinear Analyses, *Journal of Japan Society of Civil Engineers*, No. 696, I-58, pp. 99–110, 2002 (in Japanese).
- 9) Hiramatsu, T., Sato, H. and Kondo, M.: Influence of Damping Factor on Earthquake Response of Arch Dam, *the 72<sup>th</sup> Annual Meeting Proceedings of Japan Society of Civil Engineers*, I-547, pp. 1093–1094, 2017 (in Japanese).

- 10) Ueda, M., Toyoda, Y., Shiojiri, H. and Sato, M.: Resonant Frequency of Concrete Arch Dam Evaluated from Observational In-Situ Records and Effects of Contraction Joints on These Features, *Journal of Japan Society of Civil Engineers*, No. 654, I-52, pp. 207–221, 2000 (in Japanese).
- 11) Watanabe, H., Razab, D. S., Takashima K. and Taniyama, H.: Interaction of Material Nonlinearity and Joint Opening on the Seismic Response of a Concrete Arch Dam, *Journal of Japan Society of Dam Engineers*, Vol. 10, No. 4, pp. 276–288, 2000 (in Japanese).
- 12) Ariga, Y., Cao, Z. and Watanabe, H.: Study on 3-D Dynamic Analysis of Arch Dam against Strong Earthquake Motion Considering Discontinuous Behavior of Joints, *Journal of Japan Society of Civil Engineers*, No. 759, I-67, pp. 53–67, 2004 (in Japanese).
- 13) Kimata, H., Horii, H. and Yazdani, M.: Seismic Safety Evaluation of Concrete Arch Dam against Earthquake-Induced Failure of Joint Rock Foundations, *Journal of Japan Society of Civil Engineers*, SER. A1 (Structural Engineering & Earthquake Engineering), Vol. 69, No. 4, pp. I\_9–I\_19, 2013 (in Japanese).
- 14) Ariga, Y.: Suggestion for Disaster Prevention Performance of Existing Dam and Verification of Performance Evaluation Method by 3-D Reproduction Analysis, *Proceedings of the Sixth Japan Conference on Structural Safety and Reliability*, FM4-7A, pp. 805–812, 2007 (in Japanese).
- 15) Ariga, Y.: 3-D Reproduction Analysis for Actual Earthquake Behaviors of Existing Dams Based on Earthquake Observation Records, *Journal of Japan Association for Earthquake Engineering*, Vol. 7, No. 2, pp. 130–143, 2007 (in Japanese).
- 16) Nakamura, S., Shiojiri, H., Ueshima, T., Ariga, Y. and Ominato, S.: Identification of Dynamic Characteristics of an Existing Arch Dam Based on Ambient Vibration and Three-Dimensional Finite Element Analysis, *Journal of Japan Society of Civil Engineers*, SER. A1 (Structural Engineering & Earthquake Engineering), Vol. 69, No. 4, pp. I\_742–I\_749, 2013 (in Japanese).
- 17) Hayasaka, T., Ariga, Y., Kawakami, K., Ueshima, T., Nakamura, S. and Shiojiri, H.: Evaluation of Dynamic Deformation Property of Arch Dam based on Earthquake Observation Results during the 2011 off the Pacific Coast of Tohoku Earthquake, *the 68<sup>th</sup> Annual Meeting Proceedings of Japan Society of Civil Engineers*, I-020, pp. 39–40, 2013 (in Japanese).
- 18) Ariga, Y., Hayasaka, T., Kawakami, K., Ueshima, T., Nakamura, S. and Shiojiri, H.: Study on Seismic Safety of Arch Dam during the 2011 off the Pacific Coast of Tohoku Earthquake by 3-D Dynamic Analysis, *the 68<sup>th</sup> Annual Meeting Proceedings of Japan Society of Civil Engineers*, I-019, pp. 37–38, 2013 (in Japanese).
- 19) Ariga, Y., Ueshima, T., Nakamura, S. and Shiojiri, H.: Seismic Safety Evaluation for Double Arch Dam during the 2011 off the Pacific Coast of Tohoku Earthquake by Three-Dimensional Dynamic Analysis, *Journal of Japan Society of Civil Engineers*, SER. A1 (Structural Engineering & Earthquake Engineering), Vol. 70, No. 4, pp. I\_121–I\_129, 2014 (in Japanese).
- 20) Ueshima, T., Kanazawa, K., Murakami, K., Nakamura, S., Shiojiri, H. and Ariga, Y.: System Identification, Detection of Proper Frequency Variation of Aged Arch Dam and Vibrational Behavior during the 2011 off the Pacific Coast of Tohoku Earthquake by Means of Long-Term Continuous Observation of Ambient Vibration/Seismic Motion, *Journal of Japan Society of Civil Engineers*, SER. A1 (Structural Engineering & Earthquake Engineering), Vol. 68, No. 4, pp. I\_186–I\_193, 2012 (in Japanese).
- 21) Japan Society of Civil Engineers: Standard Specifications for Concrete Structures–2002 (Seismic Performance Verification), p. 47, 2002 (in Japanese).

**(Original Japanese Paper Published: January, 2020)**  
**(English Version Submitted: December 10, 2021)**  
**(English Version Accepted: January 11, 2022)**